A Closed-Form Integral Model of Spiral Inductor Using the Kramers–Kronig Relations

C. C. Chen, J. K. Huang, and Y. T. Cheng, *Member, IEEE*

***Abstract*—In this letter, a closed-form integral model is presented for the rectangular micromachined spiral inductor. The Kramers–Kronig relations provide an elegant theory to describe the inductor behavior without having complicated geometric analysis. Simulation and measurement results validate that the model can provide satisfactory prediction to the inductance of on-chip freely-suspended spiral inductors. Meanwhile, unlike conventional Greenhouse-based formulations, the self-resonant frequency of inductor can be predicted using the integral model.**

***Index Terms*—Kramers–Kronig relations, radio frequency integrated circuit (RFIC), self-resonant frequency, spiral inductor.**

I. Introduction

SPIRAL inductors have been developed and widely used for radio frequency integrated circuit (RFIC) designs. Their related characteristics, including inductance, quality factor, self-resonant frequency, and loss mechanism etc., have already been investigated in detail. A variety of methodologies to calculate the inductance of a spiral inductor, such as Greenhouse-based formulations [1]–[3], empirical expressions [4], and analysis and simulation of inductors and transformers in integrated circuits (ASITIC) [5], have been presented for the design applications. Nevertheless, in order to facilitate the implementation of integrated inductors, a compact scalable physical model that can accurately predict the behaviors of the inductors with different technologies' parameters is still an important research topic for the RFIC design and optimization [4], [6]–[9].

Conventional inductor models [6]–[8] could calculate inductance precisely. The applied method, however, is based on the Greenhouse algorithm [1]. Though the algorithm is very accurate, it still employs numerous summation steps that depend on the number of interacting segments and overall combinations of parallel segments. Meanwhile, there are nonphysical expressions, obtained using a large number of fitting factors. Since the factors are created to overcome the imperfect of the fitting function, it is essential to create an accurate mathematical expression based on the physical sense for the inductance calculation. In this letter, we will present a mathematical model based on the Kramers–Kronig relations [10]–[12] to characterize a spiral inductor in which RFIC designers could easily have the optimal design using this analytical method.

Manuscript received April 4, 2005; revised July 12, 2005. This work was supported in part by the National Science Council of Taiwan, R.O.C. under Grant NSC 92-2220-E-009-006 and by the MediaTek Research Center. The review of this letter was arranged by Associate Editor M. Mrozowski.

The authors are with Microsystems Integration Laboratory, Department of Electronics Engineering, National Chiao Tung University, Hsinchu 300, Taiwan, R.O.C. (e-mail: ytcheng@mail.nctu.edu.tw).

Digital Object Identifier 10.1109/LMWC.2005.859019

II. Constitutive Formulation

A. Determination of the Kramers–Kronig Relations

The Kramers–Kronig relations compose one of the most elegant and general theorems in physics because their validity only depends on the principle of causality: the response cannot come before the stimulation. Therefore, the relations are powerful enough to analyze the mathematically and physically conjugated phenomenon. Based on the Riemann–Lebesgue lemma and the characteristic of a conducting medium, the Kramers–Kronig relations could be built up as the form of the susceptibility, χ, as the following [10]:

$$\mathrm{Re}\chi(\omega) = \pi\sigma_0\delta(\omega) + \frac{2}{\pi}P\int_0^\infty d\omega' \frac{\omega'\mathrm{Im}\chi(\omega')}{\omega'^2-\omega^2} \quad (1)$$

$$\mathrm{Im}\chi(\omega) = \frac{\sigma_0}{\omega} - \frac{2}{\pi}P\int_0^\infty d\omega' \frac{\omega\mathrm{Re}\chi(\omega')}{\omega'^2-\omega^2} \quad (2)$$

where σ_0 is the dc conductivity of metal, ω is the frequency of electromagnetic (EM) field in the system, and P stands for principle part. The concurrence relationship of the real and image parts of a physical function are then built up to explain certain characteristics.

For instance, preceded with the Lorentz–Drude Model (1900) in a conducting medium [10], [11] a phenomenon called anomalous dispersion occurring near a narrow absorption feature, i.e., resonant absorption in a metal vapor, can be well represented in terms of the utilization of (1) and (2) to describe the relation between resonant absorption and anomalous dispersion. The dispersion and absorption are coupled and associated with the real and imaginary parts of the susceptibility, respectively. If a medium has an imaginary component of the susceptibility at the self-resonant frequency, it must have a real component over a broad range of frequencies around the self-resonant frequency. While the resonance occurs, the energy of incident EM wave is fully absorbed by the free electrons inside the medium and the absorption is peaked strongly at the resonant frequency.

Similar physical behavior of the resonance is also applicable for the case of a spiral inductor. The self-resonance occurrence of the spiral inductor would result in complete energy transformation from stored magnetic energy into electrical energy, vice versa. The occurrence of the energy exchange is similar to the anomalous dispersion in which the incident EM wave is totally absorbed by the conducting medium and transformed into the kinetic energy of the free electrons. Therefore, we can construct a physic-based inductor model using the Kramers–Kronig relations.

First, we assume that the inductor is perfect for EM wave signal propagation without having any energy loss. Thus, the

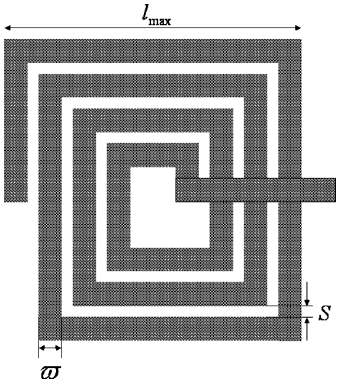

Fig. 1. Schematic diagram of the spiral inductor. $L_{\max}$, s, and ϖ are the maximum edge, line spacing, and line-width of the inductor, respectively.

imaginary part, (2), could be rationalized as a very narrow absorption of the EM wave at self-resonant frequency, ω_r, due to the energy transformation and it can be modified as

$$\mathrm{Im}\chi(\omega) \approx \frac{\sigma_0}{\omega} + \frac{\pi}{2}\frac{\alpha\delta(\omega-\omega_r)}{\omega_r} \tag{3}$$

which accompanied with the real part as the following:

$$\mathrm{Re}\chi(\omega) \approx \frac{\sigma_0}{\pi}\left[\pi^2\delta(\omega) - \frac{\ln\omega}{\omega}\right] + \frac{\alpha}{\omega_r^2-\omega^2} \tag{4}$$

where

$$\alpha = \frac{3n_e\mu_B^2\omega_r}{2\hbar} - \frac{e^2n_e(\omega_r-\omega)}{2m_e}\sum_{m=0}^{[n-1]}(l_{\max}-2ms)^2. \tag{5}$$

In (5), $\hbar$, μ_B, n_e, and m_e are Planck's constant, Bohr magneton, the electron density, and mass in material, respectively. For a spiral inductor with the geometry as shown in Fig. 1, the first and second terms in (5) are the paramagnetism and diamagnetism factors [12], [13] of the inductor material. The symbol $[n-1]$ represents the Gaussian symbol where n is the number of turns. The parameters, $l_{\max}$ and s, represent the maximum edge and line spacing of the inductor, respectively.

B. Determination of the Self-Resonant Frequency

In metal, the kinetic energy of free electrons can be described by the dispersion relation [10]

$$E_L = \sqrt{\frac{3}{5}}\frac{\hbar^2}{m_e}(3\pi^2n_e)^{1/3}k \tag{6}$$

where k is the wave number of free electrons. According to Jackson's theory [11], there will be electric fields built up in the neighborhood of corners while an external electric field is applied on a conducting material. Thus, for a polygon spiral inductor, the electric field built up in each corner has the form as the following that is calculated by the variation principle [14]:

$$\vec{E}(r) = \frac{1}{4\pi\varepsilon_0}\frac{q\left[\pi+8\sin\left(\frac{\pi^2}{4\beta}\right)\right]^2}{2\varpi h\left[\csc\left(\frac{\beta}{2}\right)-1\right](\pi+\beta)}\hat{r} \tag{7}$$

where q, β, ϖ, and h are elementary charge ($\sim 1.6\times10^{-19}$ C), the corner angle, and the width and height of the spiral inductor, respectively. The field center is assumed at the outer apex of each corner. By considering the Compton Effect [15], [16], free electrons moving near the corner would be scattered by the electric field to change their trajectories. Thus, the energy loss of the scattered electron is calculated as the following:

$$E_C = \frac{\pi\varepsilon_0\varpi h\left[\csc\left(\frac{\beta}{2}\right)-1\right]\left|\vec{E}\right|q}{NV^{2/3}\sqrt{\sigma_{\mathrm{eff}}}}\csc^2\left(\frac{\pi-\beta}{2}\right) \tag{8}$$

where N, V, and σ_{eff} are the number of corners, the volume of polygon spiral inductor, and the effective cross section of the inductor, respectively. Here, the effective cross sections are equal to 0.101 and 0.281 times the cross section, A, of rectangular and octagonal inductors, respectively.

Since the built-up electric field would alter the forward direction of the free electrons and possibly make the electrons move straight to the end of the inductor, the concept of standing wave in a cavity can be safely implemented in this model. We assume that, while resonating, the electrons could absorb the magnetic energy of the EM wave to form electric energy by forming standing waves inside the inductor and the corresponding k is equal to π/l_{total} where l_{total} represents the total length of the inductor. Thus, the self-resonant frequency of the inductor would be the same as the frequency of the resonating electron and be calculated by energy conservation as the following:

$$\omega_r = \frac{(E_L + N\cdot E_C)}{\hbar}. \tag{9}$$

The electron energy is equal to the kinetic energy plus the total energy lost in the corner field scattering.

C. Determination of the Inductance

The inductance can be derived from the associated magnetic energy of EM field in the inductor [10]

$$L \equiv \frac{\int\vec{H}^*\cdot\vec{B}dv}{I^2} \approx \mu_0 d(1+\mathrm{Re}\,\chi(\omega)) \tag{10}$$

where

$$d = \frac{n_e{l_{\mathrm{total}}}^3\hbar\omega_r}{2\pi\sigma_0^2An}\left[\exp\left(\frac{\hbar(\omega-\omega_r)}{k_BT}\right)+1\right]^{-1} \tag{11}$$

where k_B and T are the Boltzmann's constant and absolute temperature, respectively.

III. Model Validation and Discussions

The model is examined by comparing with the contemporary calculations [2], [17] including the results derived from the Greenhouse-based model and Ansoft-HFSS simulator, respectively. Meanwhile, the accuracy of HFSS analysis in this letter is experimentally validated. Fig. 2 shows good S-parameter match between the measurement and HFSS simulation in a Smith chart. The measured device is an on-chip 3.5 turns, 5-μm-thick micromachined copper spiral inductor with $l_{\max}=$ 300 μm, $s=5$ μm, and $\varpi=15$ μm as shown in Fig. 2(b). Since the substrate coupling effect is not included in this model at this moment, the micromachined type inductor is the best test

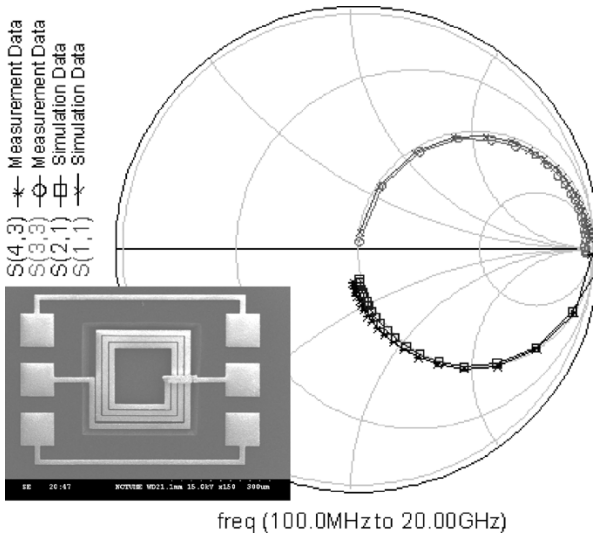

Fig. 2. Comparison between the HFSS simulation and measurement results of the 3.5 turns, 5 μm thick suspended spiral inductor. A SEM micrograph on lower left hand side shows the measured on-chip micromachined spiral inductor. The silicon substrate underneath the inductor is removed.

TABLE I
COMPARISON RESULTS

Number of Turns Comparisons (n)	1.5	2.5	3.5	4.5	5.5
ω_r for HFSS (GHz)	39.5	27.1	22.9	20.6	19.4
ω_r for K. K. model (GHz)	38.6	28.6	23.9	21.4	19.9
ω_r for Greenhouse (GHz) based model [2]	X	X	X	X	X
L for HFSS @ 3GHz (nH)	1.58	2.94	4.27	5.31	6.01
L for K. K. model @ 3GHz (nH)	1.18	2.65	4.13	5.32	5.95
L for Greenhouse-based model @ 3GHz (nH)* [2]	1.60	3.02	4.28	5.18	5.60
L for HFSS @ 5GHz (nH)	1.58	2.99	4.38	5.49	6.21
L for K. K. model @ 5GHz (nH)	1.19	2.71	4.25	5.51	6.20
L for HFSS @ 9GHz (nH)	1.63	3.22	4.92	6.31	7.23
L for K. K. model @ 9GHz (nH)	1.24	2.91	4.74	6.33	7.30

Symbol definition:
(1) K. K. model means the model developed in this paper using Kramers-Kronig relations
(2) X represents NOT available.
(3) ω_r represents the self-resonant frequency of spiral inductor.
(4) L represents the inductance of spiral inductor.
(5) In the analysis, the geometry of the inductor is designed as l_{max}= 300μm, s=5μm, and ϖ=15μm, respectively. The material utilized here is copper with the properties of, $n_e = 8\text{x}10^{28}$ m^{-3}, m_e=9.11x10^{-31} kg, and σ= 5.6x10^7 (Ωm)$^{-1}$.
* Greenhouse model does not provide the frequency dependence of the inductance

vehicle to examine this model. In comparison with the other calculations as listed in Table I, this closed-form integral can provide a very closely prediction with less than 4% relative deviation while the number of turns is larger than 2.5. Besides, the integral also reveals the relations between the inductor characteristics and the geometric factors and material properties of inductor. These physical parameters will allow us to optimize the inductor design.

At present, the integral can only well simulate the behaviors of micromachined inductor and has its potential applications for the design of high performance RFICs due to the high Q characteristic of the inductor [18], [19]. However, we think that the integral can be further modified for general on-chip inductors by considering the affectations of the diamagnetism factor and self-resonant frequency resulted from the substrate coupling effect.

IV. CONCLUSION

Our analytical method creates a closed-form integral which could predict the inductance and self resonant frequency of a micromachined spiral inductor. The inductance expression is closely fitted with the simulation and experimental data for the structure of the spiral inductor with substrate removal. The analytical method based on the Kramers–Kronig relations and EM field theory could provide mathematical convenience for the inductor design in a physical sense.

REFERENCES

[1] H. M. Greenhouse, "Design of planar rectangular microelectronic inductor," *IEEE Trans. Parts, Hybrids, Packag.*, vol. PHP-10, no. 2, pp. 101–109, Jun. 1974.
[2] S. Jenei, B. K. J. C. Nauwelaers, and S. Decoutere, "Physics-based closed-form inductance expression for compact modeling of integrated spiral inductors," *IEEE J. Solid-State Circuits*, vol. 37, no. 1, pp. 77–80, Jan. 2002.
[3] S. Asgaran, "New accurate physics-based closed-form expressions for compact modeling and design of on-chip spiral inductors," in *Proc. 14th Int. Conf. Microelectronics*, Dec. 2002, pp. 247–250.
[4] S. S. Mohan, M. M. Hershenson, S. P. Boyd, and T. H. Lee, "Simple accurate expressions for planar spiral inductance," *IEEE J. Solid-State Circuits*, vol. 34, no. 10, pp. 1419–1424, Oct. 1999.
[5] A. M. Niknejad and R. G. Meyer, *Design, Simulation and Applications of Inductors and Transformers for Si RF ICs*. Boston, MA: Kluwer, 2000.
[6] S. S. Mohan, M. M. Hershenson, S. P. Boyd, and T. H. Lee, "Simple accurate expressions for planar spiral inductance," *IEEE J. Solid-State Circuits*, vol. 34, no. 10, pp. 1419–1424, Oct. 1999.
[7] Y. Koutsoyannopoulos *et al.*, "A generic CAD model for arbitrary shaped and multilayer integrated inductors on silicon substrates," in *Proc. ESSDERC'97*, 1997, pp. 320–323.
[8] J. R. Long and M. A. Copeland, "The modeling, characterization and designed monolithic inductors for silicon RF ICs," *IEEE J. Solid-State Circuits*, vol. 32, no. 3, pp. 357–369, Mar. 1997.
[9] A. M. Niknejad and R. G. Meyer, "Analysis, design and optimization of spiral inductors and transformers for Si RF ICs," *IEEE J. Solid-State Circuits*, vol. 33, no. 10, pp. 1470–1481, Oct. 1998.
[10] C. A. Brau, *Modern Problems in Classical Electrodynamics*. New York: Oxford Univ., 2004.
[11] J. D. Jackson, *Classical Electrodynamics*. New York: Wiley, 1998.
[12] C. Kittel, *Introduction to Solid State Physics*, 7th ed. New York: Wiley, 2004.
[13] N. W. Ashcroft and N. D. Mermin, *Solid State Physics*. New York: Holt-Sanders, 1976.
[14] G. B. Arfken and H. J. Weber, *Mathematical Methods for Physicists*. New York: Academic, 2005.
[15] A. S. Kronfeld and B. Nižić, "Nucleon compton scattering in perturbative QCD," *Phys. Rev. D.*, vol. 44, pp. 3445–3465, 1991.
[16] F. J. Federspiel, R. A. Eisenstein, M. A. Lucas, B. E. MacGibbon, K. Mellondorf, A. M. Nathan, A. O'Neill, and D. P. Wells, "Proton compton effect: A measurement of the electric and magnetic polarizabilities of the proton," *Phys. Rev. Lett.*, vol. 67, pp. 1511–1514, 1991.
[17] Ansoft. (2005) HFSS products. Tech. Rep.. [Online]. Available: http://www.ansoft.com/products/hf
[18] H. Lakdawala, X. Zhu, X. H. Luo, S. Santhanam, L. R. Carley, and G. K. Fedder, "Micromachined high-Q inductors in a 0.18-μm copper interconnect low-k dielectric CMOS process," *IEEE J. Solid State Circuits*, vol. 37, no. 3, pp. 394–403, Mar. 2002.
[19] J. Hongrui, Y. Wang, J. –L. A. Yeh, and N. C. Tien, "On-chip spiral inductors suspended over deep copper-lined cavities," *IEEE Microw. Theory Tech.*, vol. 48, no. 12, pp. 2415–2423, Dec. 2000.